eLIFE
elifesciences.org

Figures and figure supplements

RNA structures that resist degradation by Xrn1 produce a pathogenic Dengue virus RNA

Erich G Chapman, et al.

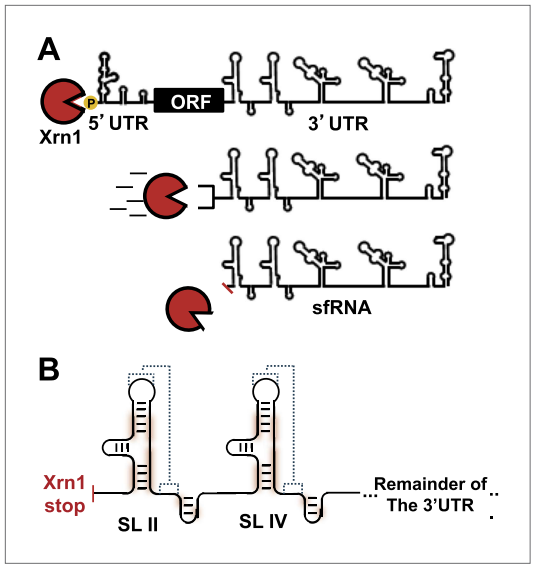

Figure 1. sfRNAs are formed by incomplete degradation of the flaviviral genomic RNA by the 5′→3′ exonuclease Xrn1. (**A**) Xrn1 (red) likely loads onto decapped, monophosphorylated gRNA and degrades ~10 kb of RNA before stopping within the viral 3′UTR. The remaining RNA is the sfRNA. (**B**) In the sfRNAs studied to date, stem-loop (SL) elements near the 5′ border of the 3′UTR/sfRNA appear to be signals for Xrn1 resistance, and are depicted here as cartoon secondary structures. In Dengue and many other FVs, two of these SLs are present in tandem, as shown. The most highly-conserved parts of the RNA are shaded red and putative PK interactions are indicated with dashed lines. Dumbbell elements (not shown) are located 3′ to these SLs.

DOI: 10.7554/eLife.01892.003

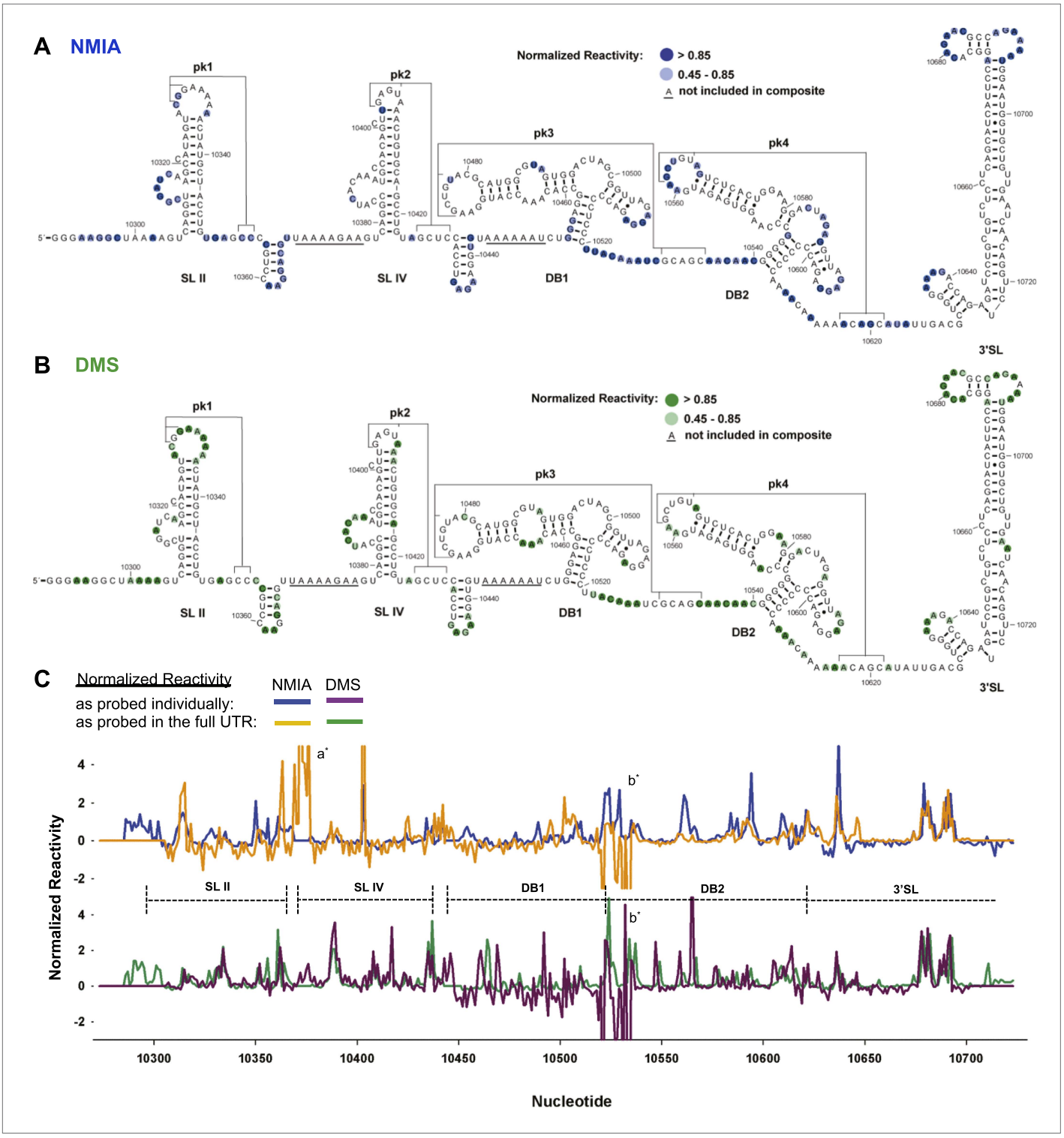

Figure 2. Chemical probing and predicted secondary structure of the DENV2 3'UTR. (**A**) The Shapeknots predicted secondary structure of the DENV2 3'UTR with NMIA reactivity data overlaid as indicated (blue). Secondary structure elements are labeled. (**B**) Same as panel (**A**), but with DMS reactivity data overlaid (green). (**C**) Chemical reactivity profiles of the DENV 3'UTR obtained when it is mapped in its entirety or a series of individually transcribed domains. The nucleotide position/number is on the x-axis, the y-axis is normalized reactivity. Locations of secondary structure elements are shown with dashed lines. An ' * ' indicates a region where the reverse transcriptase tended to stop in the full length 3'UTR. See **Supporting Information** for additional details.

DOI: 10.7554/eLife.01892.004

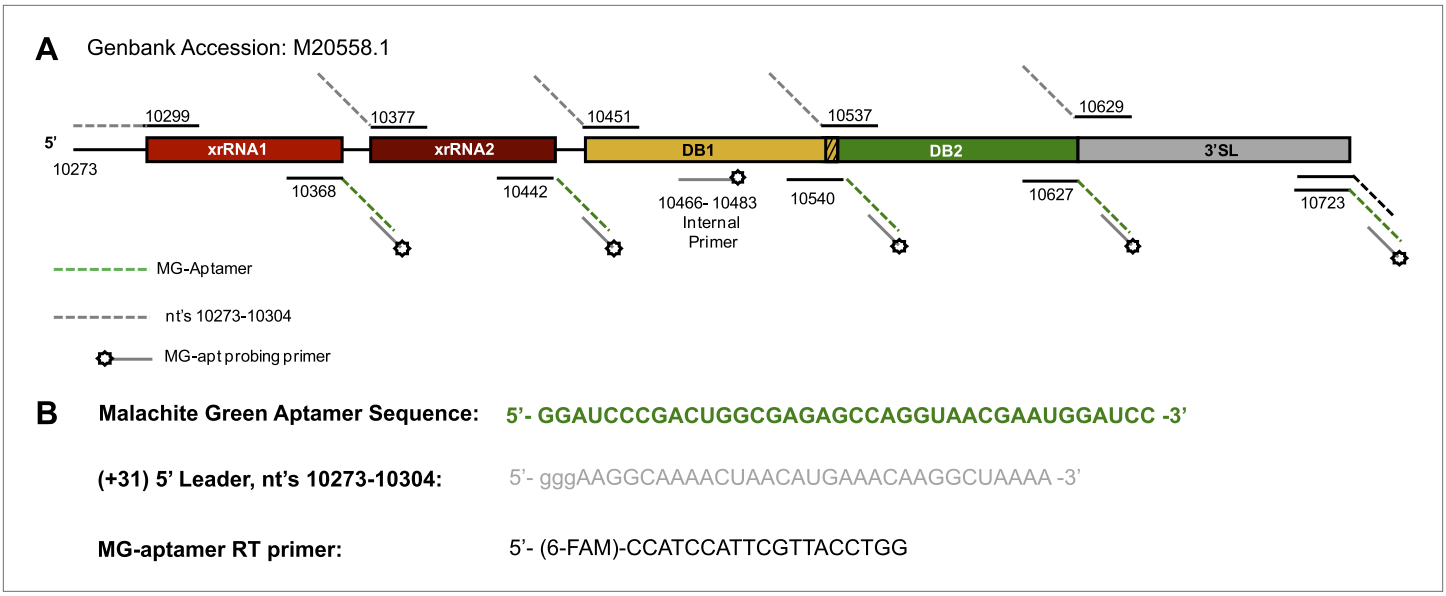

Figure 2—figure supplement 1. Map of the RNAs used during the chemical probing experiments described in this work.

DOI: 10.7554/eLife.01892.005

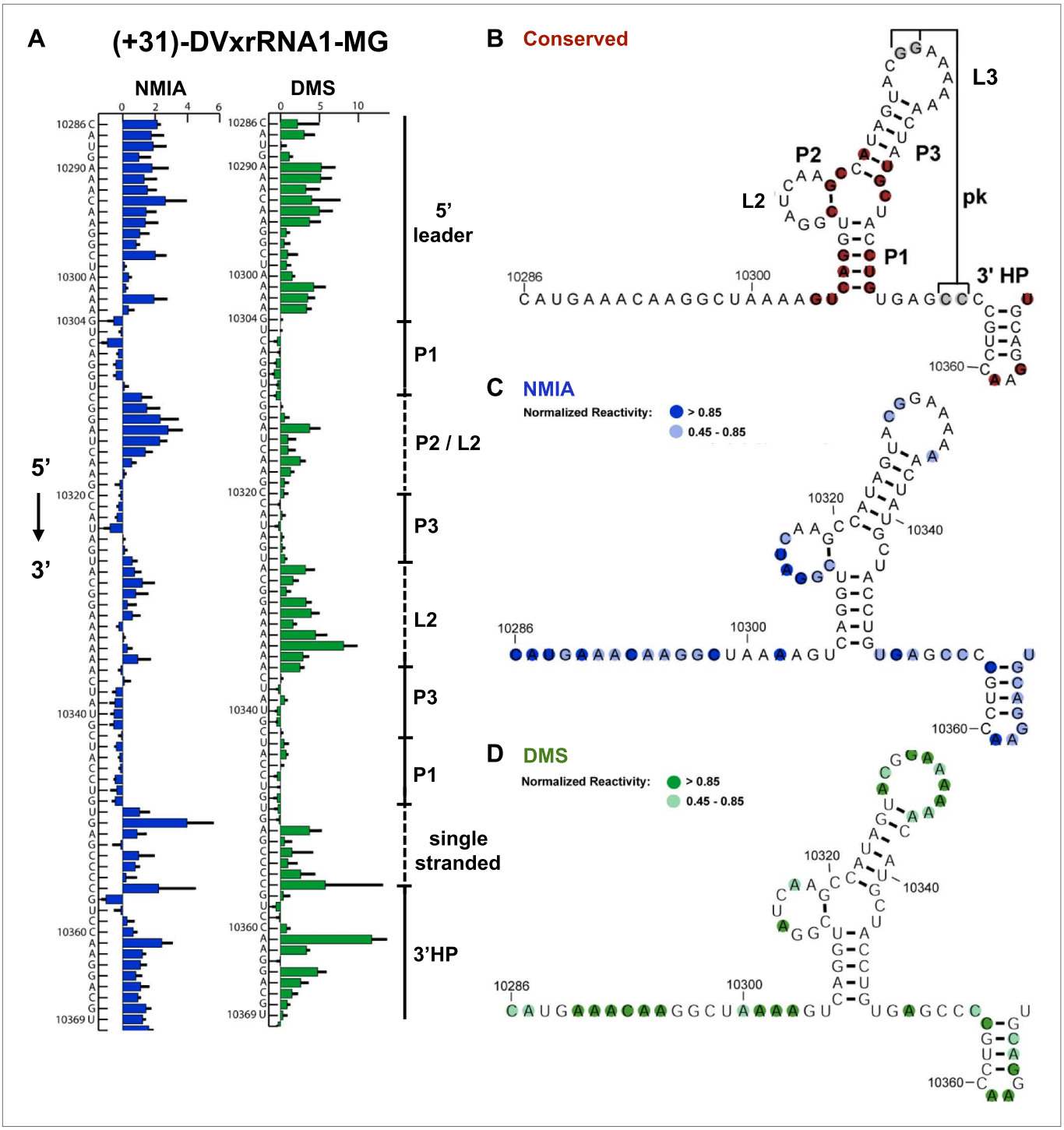

Figure 3. Refined secondary structure of SLII RNA in the DENV2 3'UTR. (**A**) Chemical probing profiles of (+31)-DVxrRNA1-MG with NMIA (blue) and DMS (green). The y-axis denotes the RNAs sequence/position, the x-axis depicts chemical reactivity. Data represent the average of three independent experiments, error bars are one standard deviation from the mean. Secondary structure elements are indicated to the right of the graphs. (**B**–**D**) Overlay of phylogenetic (**B**), NMIA (**C**), and DMS (**D**) data that support the shown refined secondary structure. In panel (**B**) secondary structure elements are labeled according to standard convention. The RNA shown here was quantitatively resistant to Xrn1 (***Figures 5B and 6D,E***).

DOI: 10.7554/eLife.01892.006

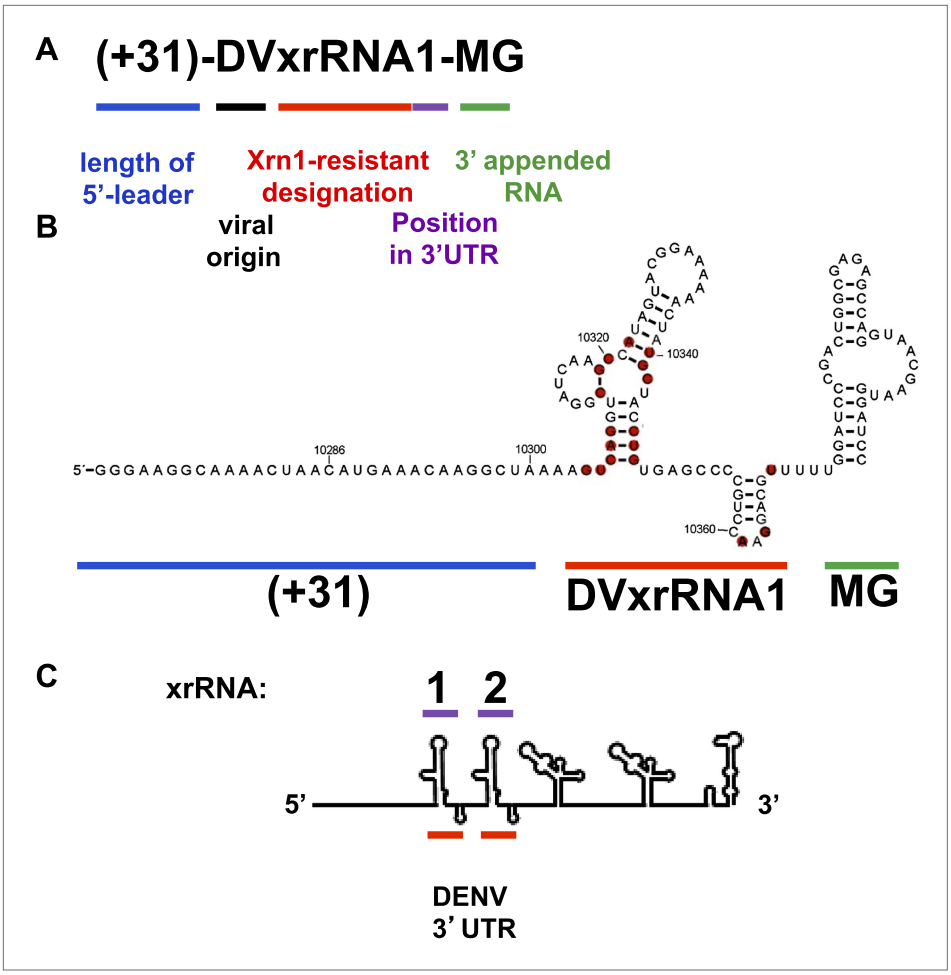

Figure 3—figure supplement 1. Naming Strategy for Xrn1-Resistant RNAs.

DOI: 10.7554/eLife.01892.007

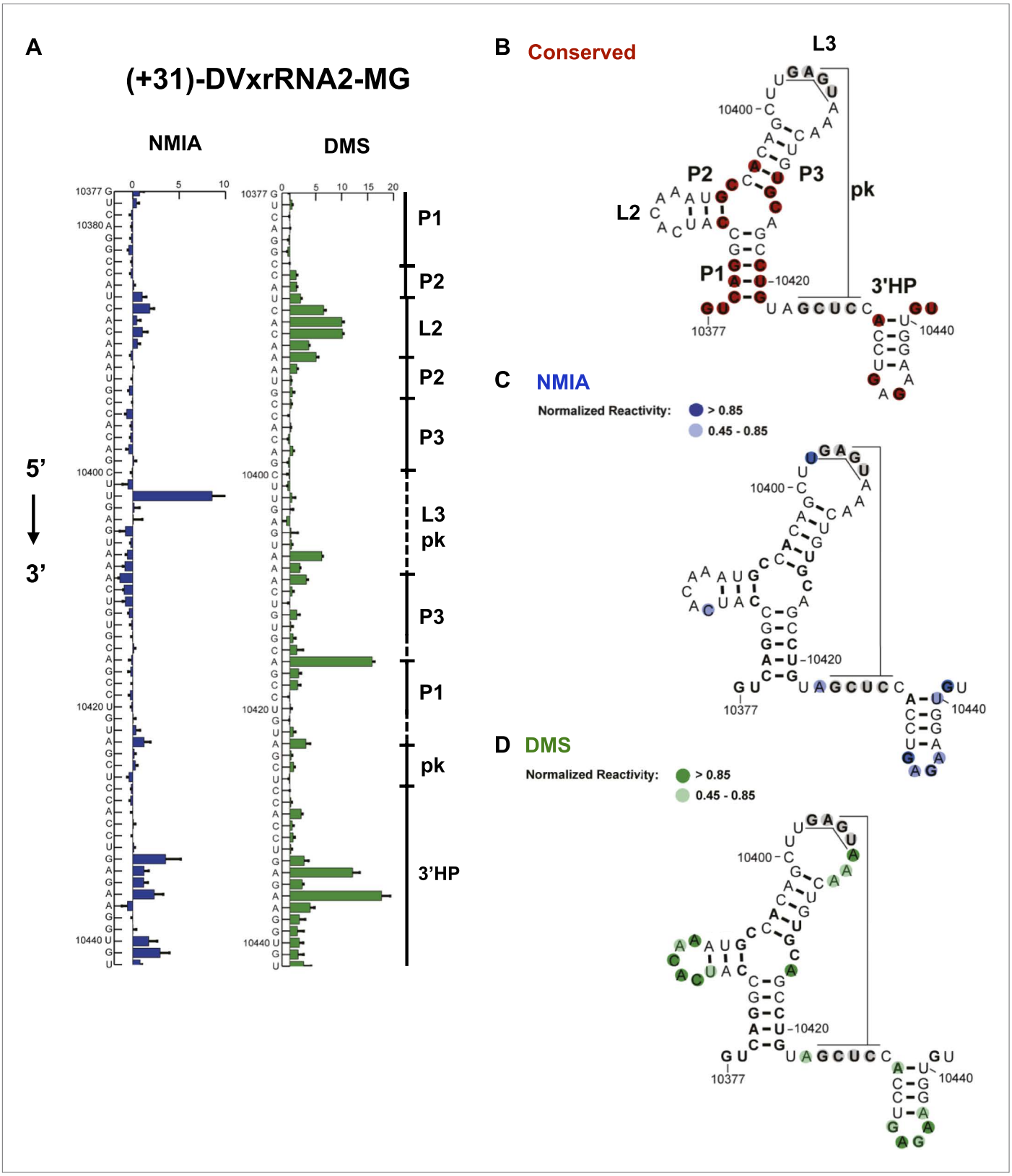

Figure 4. Refined secondary structure of SL IV RNA (DVxrRNA2) in the DENV2 3'UTR. (**A**) Chemical probing profiles of (+31)-DVxrRNA2-MG from NMIA (blue) and DMS (green) -probed RNAs. The y-axis contains the sequence and nucleotide numbers, the x-axis depicts chemical reactivity. Data represent the average of three independent experiments, error bars show one standard deviation from the mean. Secondary structure elements are indicated to

Figure 4. Continued on next page

Figure 4. Continued

the right of the graphs. (**B**–**D**) Overlay of phylogenetic (**B**), NMIA (**C**), and DMS (**D**) data the support this refined secondary structure. In panel (**B**) we assign names to the secondary structure elements according to standard convention. The RNA shown here was quantitative resistance to Xrn1 degradation (***Figure 6D,E***).

DOI: 10.7554/eLife.01892.008

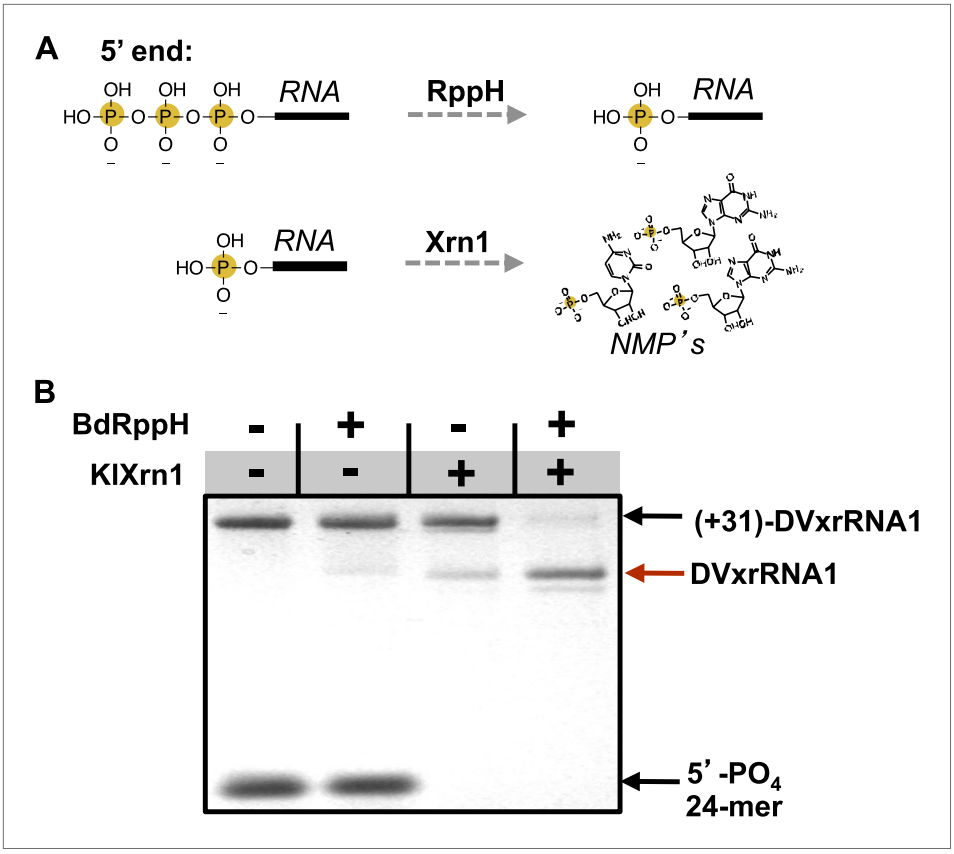

Figure 5. Recapitulation of Xrn1 resistance in vitro. (**A**) Reactions carried out by RppH and Xrn1. (**B**) Gel demonstrating the specificity of each component in the reconstituted reaction and the Xrn1-resistant behavior of (+31)-DVxrRNA1 (the input test RNA), which contains the isolated SL II element after a 31 nucleotide-long leader. The red arrow indicates the truncated product formed by Xrn1 resistance (DVxrRNA1, the resistant RNA). The 24-mer control RNA is labeled.

DOI: 10.7554/eLife.01892.009

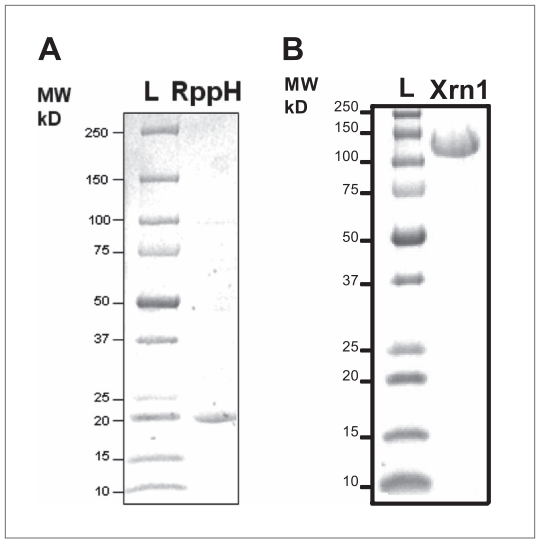

Figure 5—figure supplement 1. Purification of RNA processing enzymes.

DOI: 10.7554/eLife.01892.010

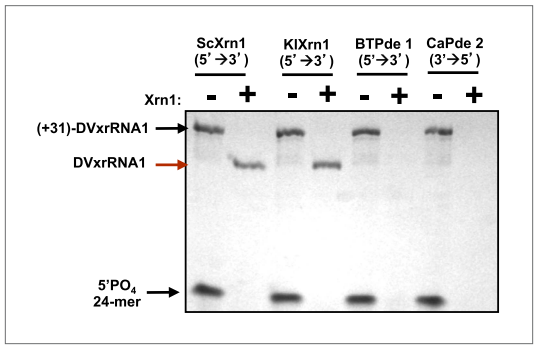

Figure 5—figure supplement 2. DVxrRNA1 demonstrates specific resistance to Xrn1.

DOI: 10.7554/eLife.01892.011

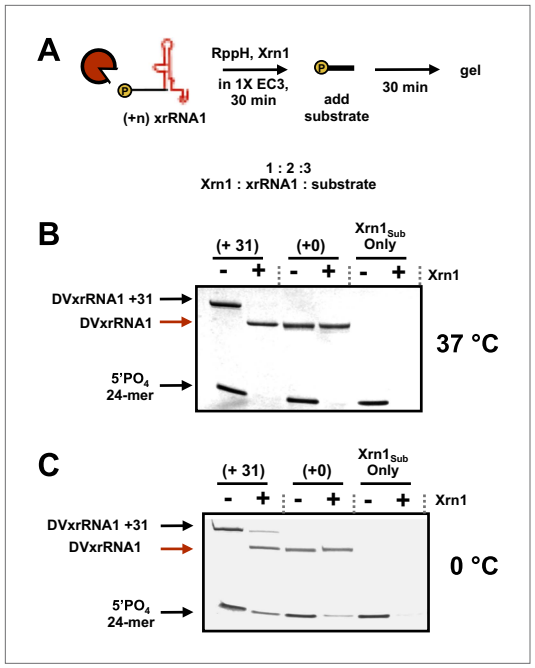

Figure 5—figure supplement 3. Examination of *in trans* protection of other Xrn1 substrates by DVxrRNA1.
DOI: 10.7554/eLife.01892.012

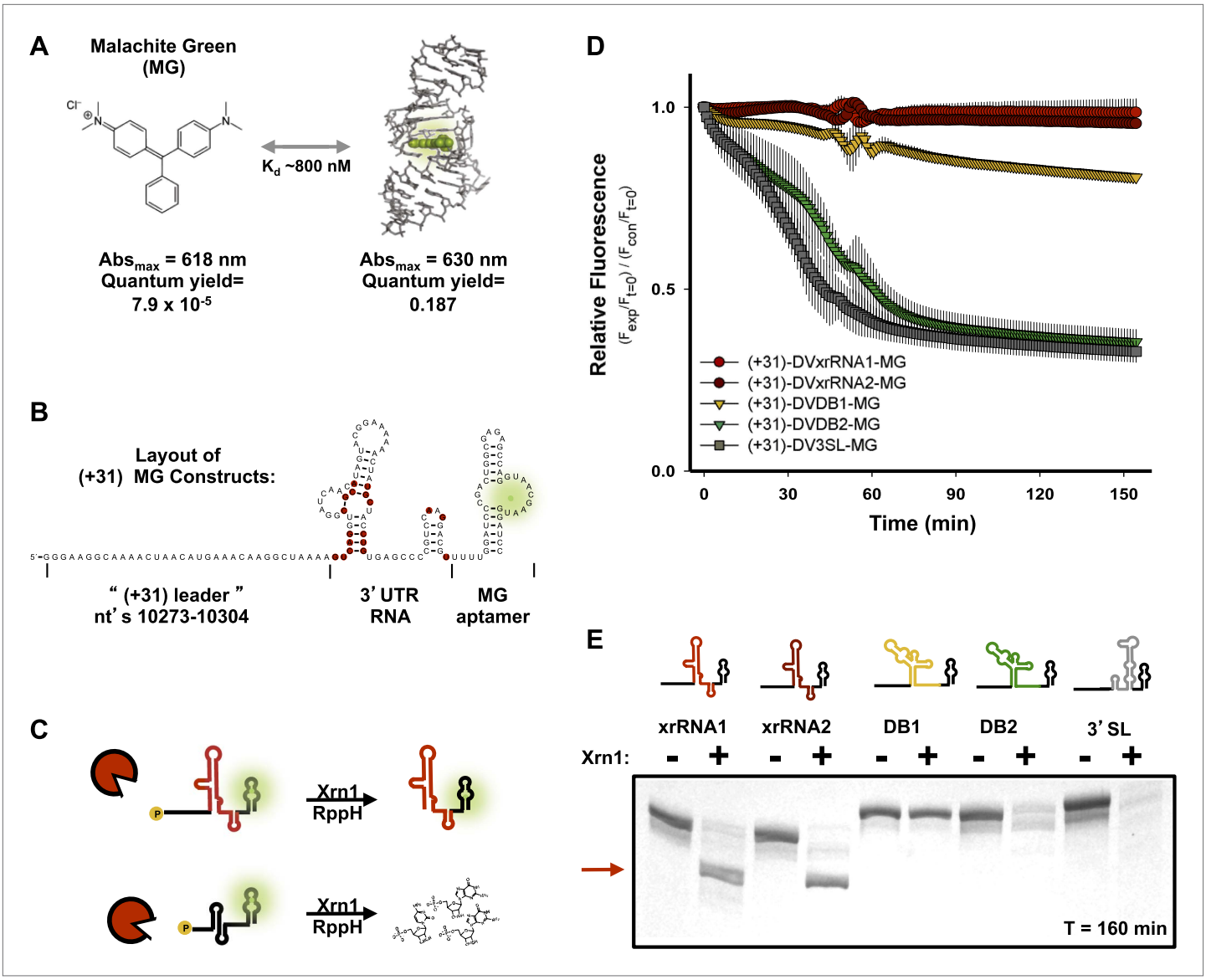

Figure 6. Design of a fluorescence assay for monitoring Xrn1 resistance and testing of individual DENV2 3′UTR structural elements. (**A**) Fluorescent properties and structure of the MG dye and MG aptamer. (**B**) Schematic of the RNA constructs used for monitoring the decay kinetics of individual elements of the DENV 3′UTR. Conserved nucleotides are colored red as in ***Figure 3B***. Green indicates fluorescing MG dye. (**C**) Cartoon representing the expected outcome when using Xrn1-resistant (top) or non-resistant (bottom) RNAs. Green glow indicates fluorescence. (**D**) Fluorescence traces of different RNAs over the course of their reaction with Xrn1. X-axis is time and y-axis is relative fluorescence intensity. Data are normalized to (−) Xrn1 controls and are averaged over three independent experiments. Error bars show one standard deviation from the mean. (**E**) dPAGE analysis of the products of the experiment of panel (**D**).

DOI: 10.7554/eLife.01892.013

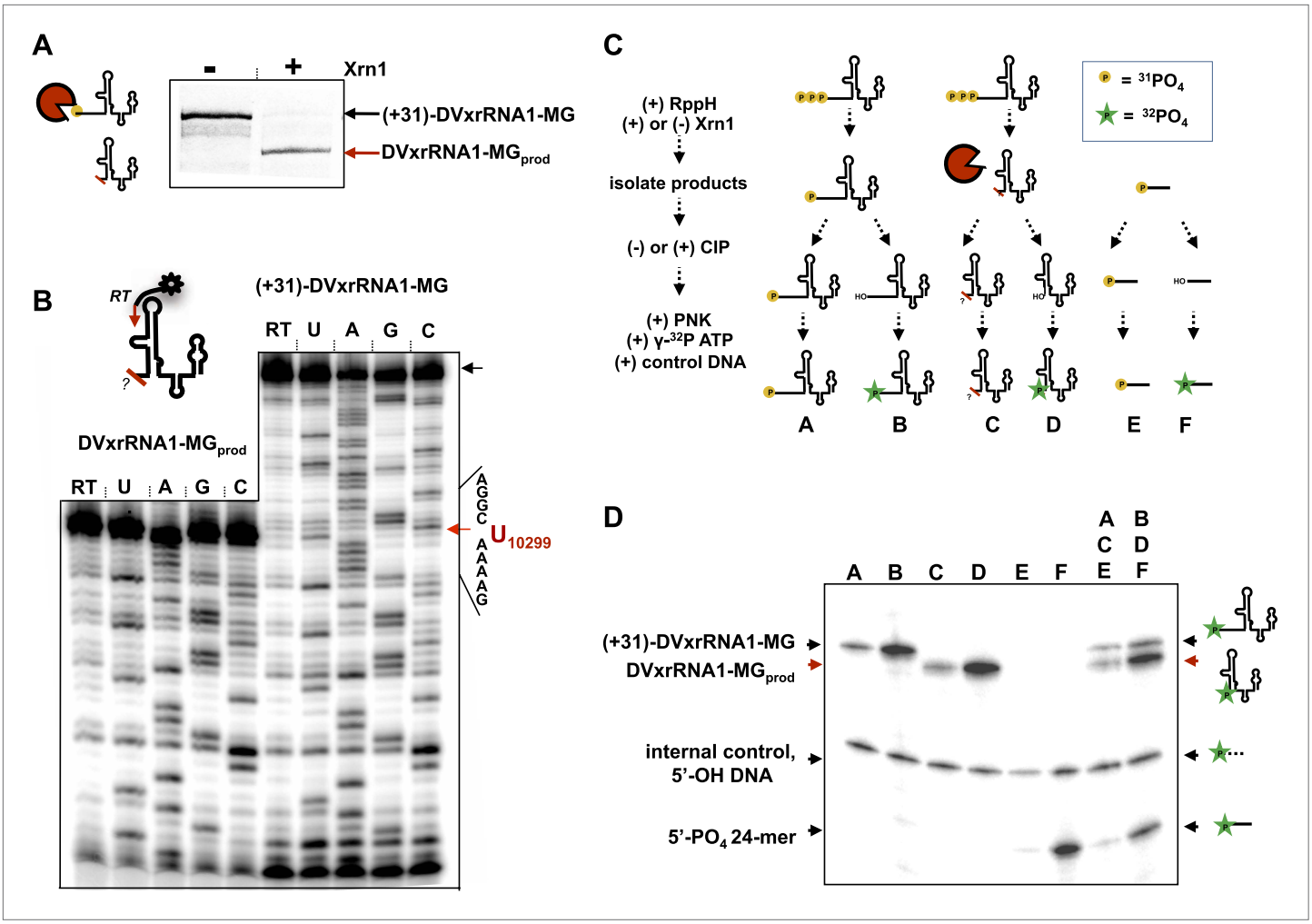

Figure 7. Characterization of the products left by Xrn1 resistance. (**A**) Gel of RNAs used to map the 5′ end of Xrn1-resistant product RNA. (**B**) Reverse transcription of RNAs from panel (**A**). The cartoon inset shows a schematic of the reaction. Dideoxy sequencing lanes are labeled. The location of the stop site (and hence the 5′ border of the product RNA) is shown with a red arrow to the right, along with the sequence of the RNA surrounding this position. (**C**) Diagram of the experiment used to determine the phosphorylation state of the products left by Xrn1 resistance. Yellow balls indicate non-radioactive phosphates, a green star depicts ^{32}P radioactive phosphates. (**D**) Gel containing the outcome of the experiment shown in panel (**C**). Different species of RNA or DNA are labeled to the left and cartooned to the right. Red arrows: Xrn1-resistant product RNA.

DOI: 10.7554/eLife.01892.014

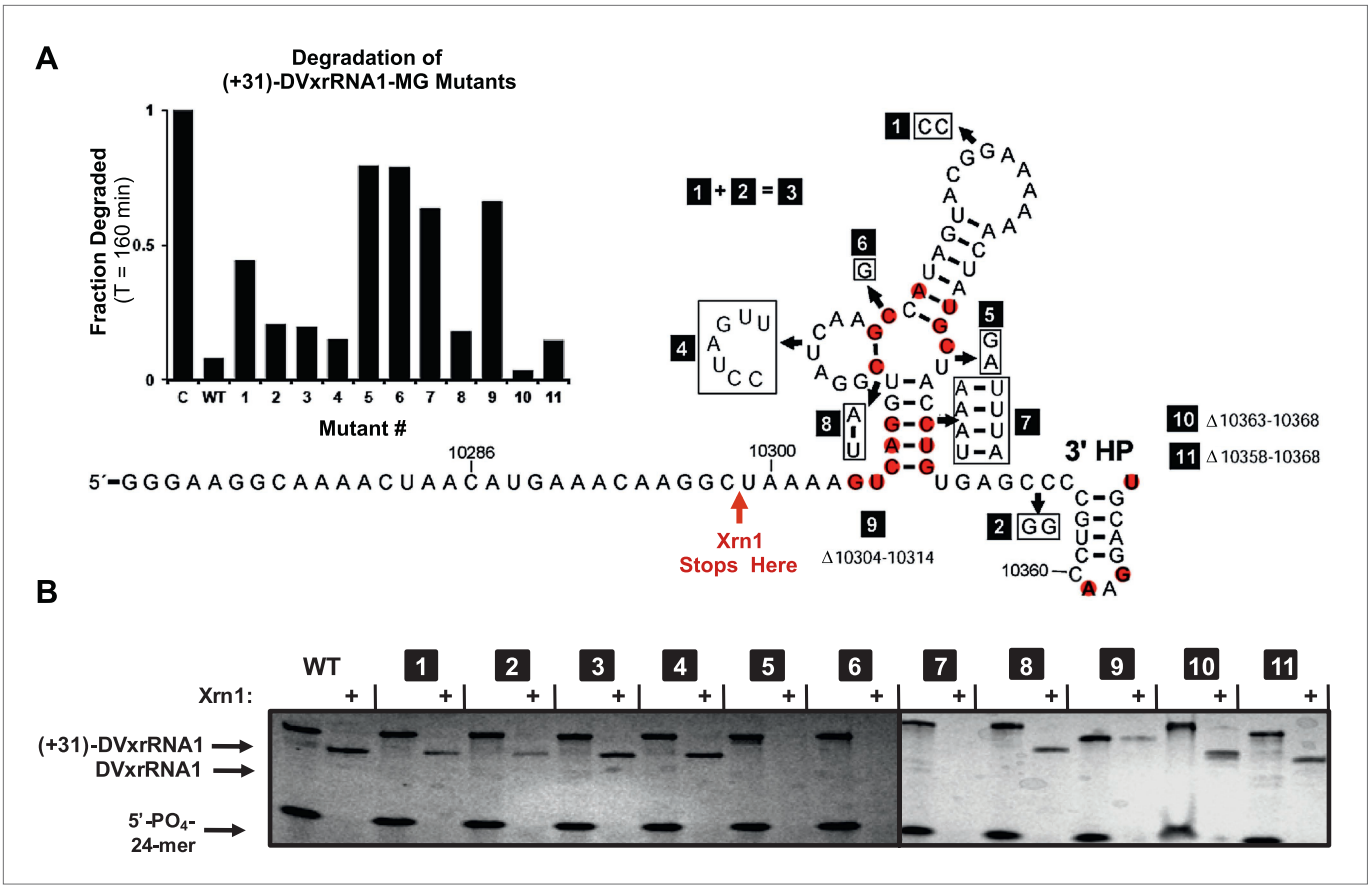

Figure 8. Mutational analysis of DVxrRNA1. (**A**) Secondary structure of DVxrRNA1 with mutations labeled Conserved sequence elements in red. The stop site for Xrn1 is indicated. Inset is a bar graph containing the effects of mutations Xrn1 resistance when quantified using the fluorescence assay. The x-axis identifies each mutant, the y-axis the fraction of MG-tagged RNA degraded at 160 min. C is a non-resistant control RNA. Graph depicts the average of two independent experiments. (**B**) Gel analysis of the reaction of each mutant with Xrn1 and RppH as in ***Figure 5***.

DOI: 10.7554/eLife.01892.015

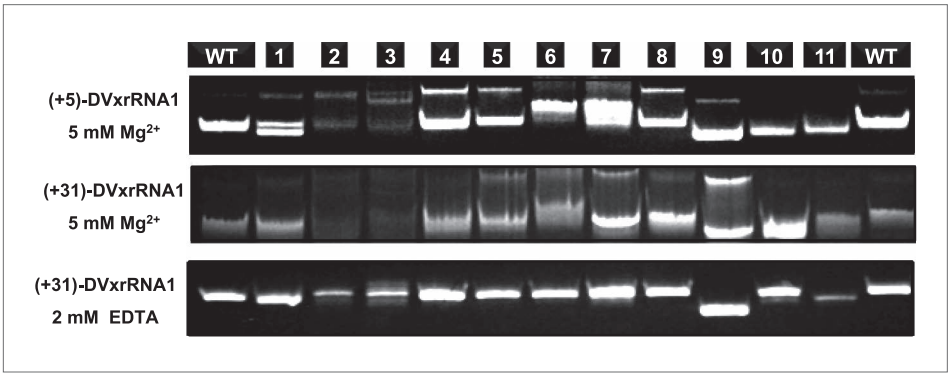

Figure 8—figure supplement 1. Native PAGE analysis of DVxrRNA1 mutants.

DOI: 10.7554/eLife.01892.016

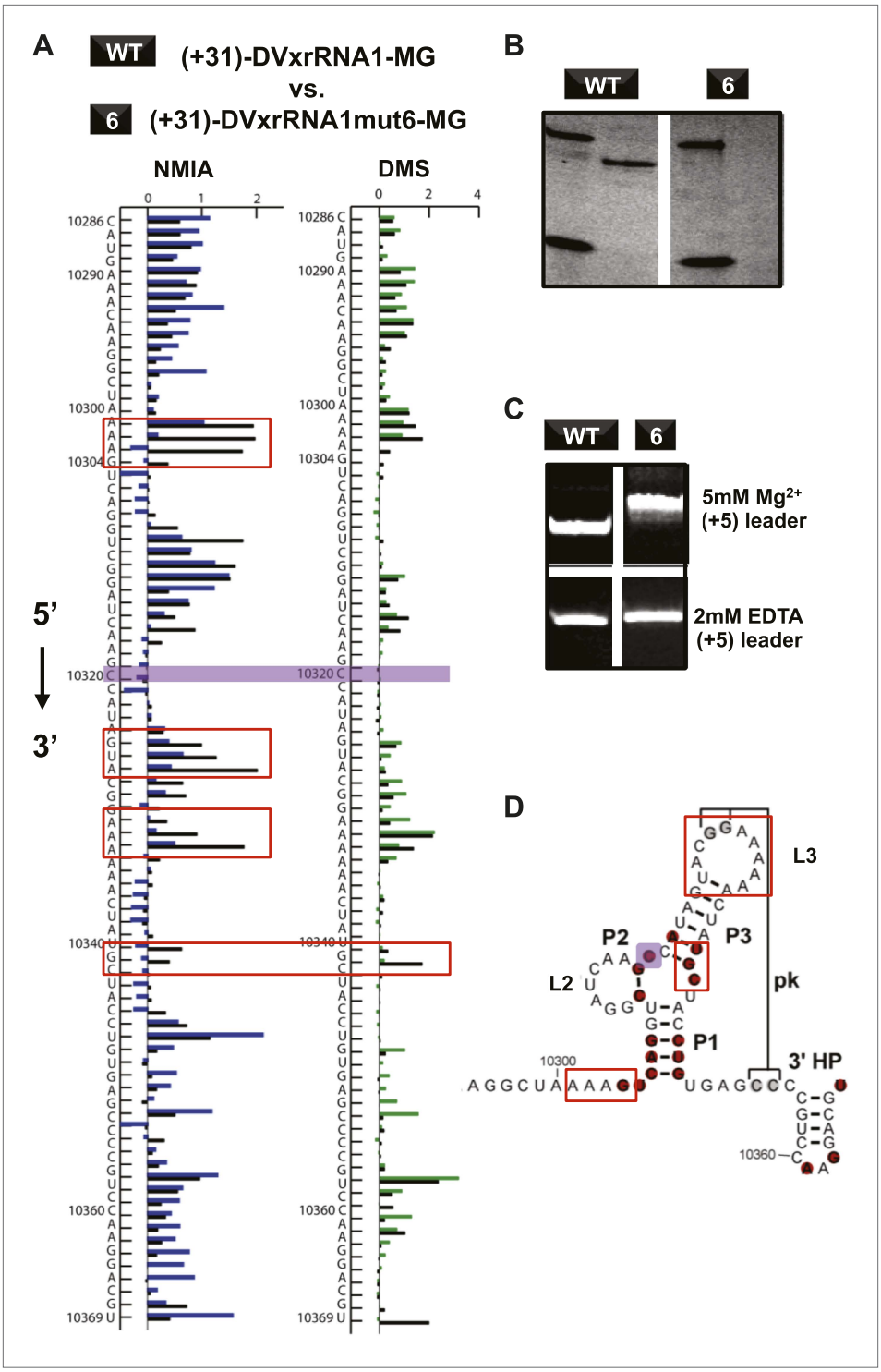

Figure 9. Structural analyses of DVxrRNA1 mutant 6 (mutant in the three-way junction). (**A**) Normalized NMIA and DMS reactivity profiles of mutant 6 compared to WT RNA, depicted as in ***Figures 3 and 4***. Colored bars (green and blue) represent the WT RNA and black bars represent mutant 6. The location of the point mutation is shown with a purple shaded box. Reactivity changes are indicated by red boxes. (**B**) dPAGE of Xrn1 resistance by WT and mutant 6. (**C**) Non-denaturing (native) PAGE analyses of WT and mutant 6. (**D**) Secondary structure of the DVxrRNA1 with elements labeled. The purple shaded box shows the location of the mutation. Regions of the structure that show substantial changes in the chemical probing (from panel (**A**)) are indicated by red boxes.

DOI: 10.7554/eLife.01892.017

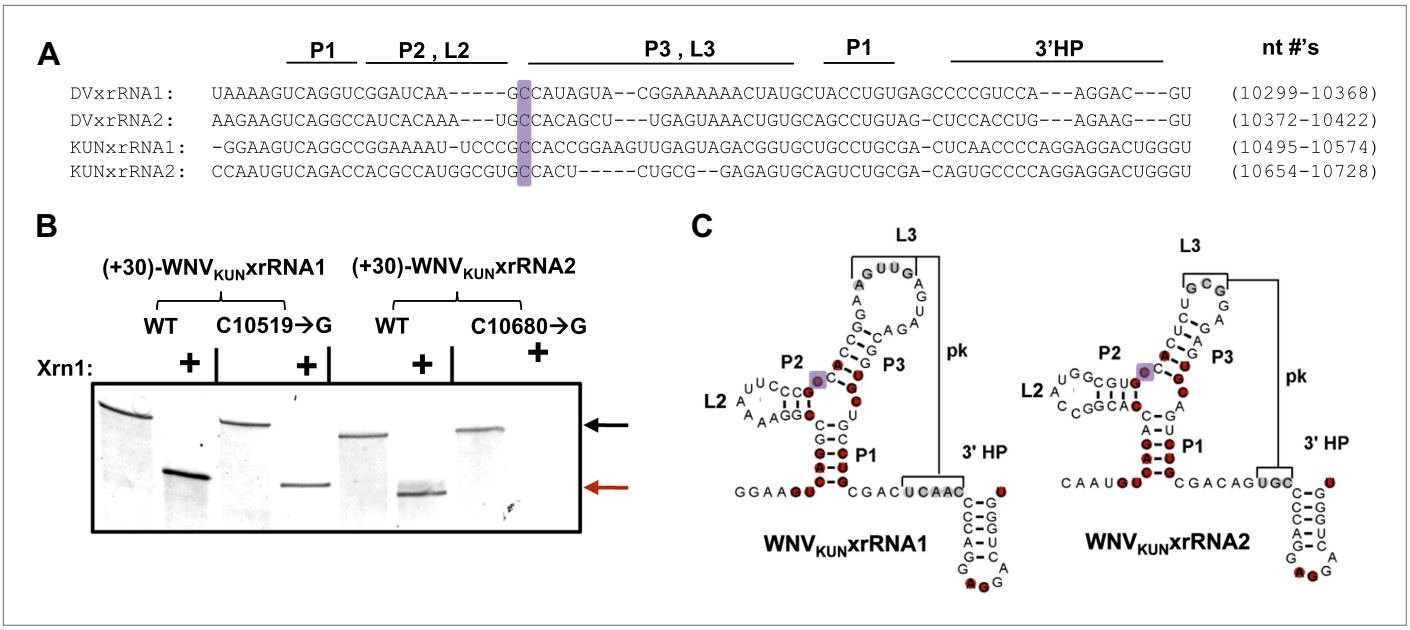

Figure 10. Identification and testing of WNV_{KUN} xrRNA structures. (**A**) Sequence alignment of DVxrRNA1, DVxrRNA2, WNV_{KUN}xrRNA1 and WNV_{KUN}xrRNA2. Nucleotide positions are indicated and correspond to Genbank accession numbers M20558.1and AY274504.1 for DENV2 and WNV_{KUN}, respectively. Conserved nucleotides of these RNAs are highlighted in red. The point mutation we made in the three-was junction is indicated with a purple box. (**B**) dPAGE of the Xrn1 resistance assay run using WNV_{KUN} xrRNAs and C10519→G and C10680→G point mutants. (**C**) Conserved secondary structure of WNV_{KUN}xrRNA1 and WNV_{KUN}xrRNA2, with conserved nucleotides highlighted and the location of the mutation shaded purple.

DOI: 10.7554/eLife.01892.018

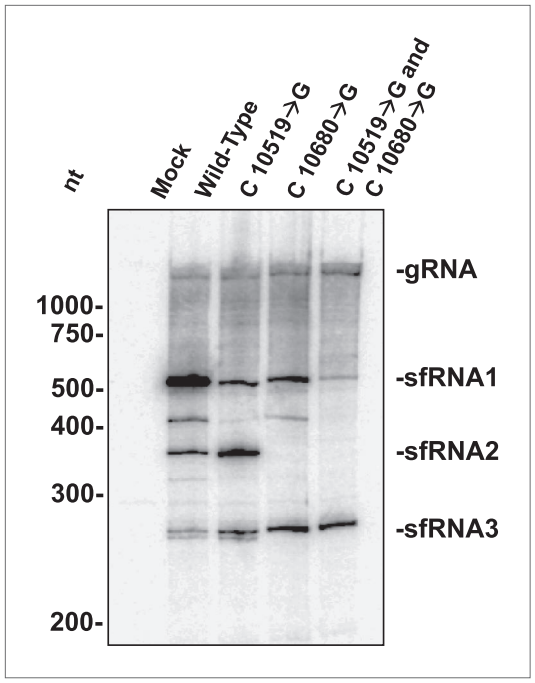

Figure 11. sfRNAs produced during infection by wild-type and mutated WNV_{KUN}. Northern blot analysis of total RNA isolated from human 293T cells infected with WT and mutants WNV_{KUN}, analyzed at 48 h.p.i. The location of molecular weight markers and the identity of sfRNA species are indicated to the left and right of the blot respectively.

DOI: 10.7554/eLife.01892.019